Enabling Resilience of Complex Engineered Systems Using Control Theory

Nita Yodo, Pingfeng Wang, *Member, IEEE*, and Melvin Rafi

***Abstract*—Successful recovery from a disrupted state to maintain optimal performance is a key feature that a resilient complex engineered system should have. In the engineering design community, the current focus of engineering resilience research is primarily directed toward improving overall system performance in the presence of likelihood failures. Little attention has been given to the study of how the system responds during and/or after the occurrence of a failure event. This paper proposes the use of control theory as a strategy to enable resilient behavior in complex engineered systems. Control theory has various benefits in its application to a resilient engineered system, with the main advantage being its ability to regulate and govern system states, even while the failure is taking place. In the context of implementation within a complex engineered system, such a controller should be designed such that, when a disturbance occurs, the controller should simultaneously be able to take timely action to correct the shift in system performance. To date, the fusion of control theory with engineering resilience has not been explored in-depth by the engineering design community. This paper, thus, presents a resilience modeling and analysis approach using fundamental control theory. The resilience of a power distribution system is employed as a case study to demonstrate the effectiveness of the proposed approach. The presented study also expects to aid in the concurrent development of resilience functions in complex engineered systems under uncertainty.**

***Index Terms*—Control theory, complex systems, engineering design, failure recovery, reliability, resilience.**

NOMENCLATURE

Acronyms and Abbreviation

DP	Desired performance.
RP	Recovery Performance.
PHM	Prognostic and health management.
PID	Proportional integral derivative.
RCES	Resilient complex engineered system.

Notation

$A(t)$	System matrix at time t.
$B(t)$	Control input matrix at time t.
$C(t)$	Output matrix at time t.
$D(t)$	Feedforward matrix at time t.
$\mathrm{DP}(t)$	Desired performance at time t.
$e(t)$	Error signal at time t.
K_d	Derivative gain constant.
K_i	Integral gain constant.
K_p	Proportional gain constant.
$P(t)$	System performance level at time t.
P_o	Initial system performance level before disruption.
P_v	System performance level after disruption.
$\mathrm{RP}(t)$	System performance recovery at time t.
T^*	Long period of time.
t_d	Occurrence time of the disruptive event.
t_n	Time to new recovered state.
t_o	Initial scenario time.
t_v	Time to vulnerable or degraded state.
$u(t)$	Control input vector at time t.
$x(t)$	System state vector at time t.
$\dot{x}(t)$	Time derivative of state vector x.
$y(t)$	Output vector at time t.
Ψ	System resilience level.

Manuscript received January 31, 2017; revised June 14, 2017; accepted August 7, 2017. Date of publication September 19, 2017; date of current version March 1, 2018. This work was supported in part by the National Science Foundation (NSF) through the Faculty Early Career Development (CAREER) award (CMMI-1351414), in part by the NSF award (CMMI-1538508), and in part by the Department of Transportation through University Transportation Center Program. Associate Editor: S. Li. *(Corresponding author: Pingfeng Wang.)*

N. Yodo is with the Department of Industrial and Manufacturing Engineering, North Dakota State University, Fargo, ND 58102 USA (e-mail: nita.yodo@ndsu.edu).

P. Wang is with the Department of Industrial and Enterprise Systems Engineering, University of Illinois at Urbana-Champaign, Urbana, IL 61801 USA (e-mail: pingfeng@illinois.edu).

M. Rafi is with the Department of Aerospace Engineering, Wichita State University, Wichita, KS 67260 USA (e-mail: mxrafi@shockers.wichita.edu).

Color versions of one or more of the figures in this paper are available online at http://ieeexplore.ieee.org.

Digital Object Identifier 10.1109/TR.2017.2746754

I. INTRODUCTION

OVER the years, many complex engineered systems have grown in terms of size and complexity. This may be attributed to the relentless pursuit of developing better, safer, and longer lasting systems that encompass a wide range of applications. Generally, a system is said to be complex if it consists of large interconnected subsystems or components which interact in diverse ways without a central organizing authority. Moreover, the individual behavior of the components does not necessarily provide the same collective behavior as the behavior of the complex system as a whole [1], [2]. These components are typically connected to become a network or a long chain structure in a complex system. Engineering systems that fall within the scope of complex systems include but are not limited to spacecraft, transportation networks, healthcare systems, production systems, and power grids.

As a system becomes more complex, it may require a new set of safety, security, and operation rules because there are more components in complex systems to be analyzed and controlled during the operational stage. In the preliminary design stage, the effect of interdependencies between the components is hard

or sometimes impossible for system engineers to fully capture [3]. This consequently challenges system designers, in the early design stage, to take account of all potential failure modes that may happen during the operational stage of the complex system. Moreover, due to the prolonged usage of a complex system, and coupled with environmental impact, new failure modes that are not anticipated at the design stage may arise in the future. Increases in complexity have directly or indirectly led the system to become more vulnerable to certain types of failures [4]. Thus, another unspoken requirement for complex systems to have a prolonged useful life is that they have to be resilient toward internal and external uncertainties and the likelihood of failures.

While past research efforts on design have been largely focused on developing a system with high reliability, there are, however, cases when high reliability is insufficient to prevent failures, especially those adverse failures caused by extreme natural disasters. The engineering resilience concept has attracted attention from system designers and researchers in addressing failures of complex engineered systems [5]. A resilient system is a system that possesses some type of failure recovery capability against likelihood failures. During the occurrence of a failure event, an RCES is expected to be able to withstand failure and maintain the same initial system performance level. If there is a negative shift in the system performance level during the aftermath of a failure event, an RCES is expected to be able to recover swiftly from its disrupted state to the original system state.

Since the failure recovery capability has to be designed into the system, the present focus of engineering resilience research is primarily directed toward improving overall system performance by incorporating various design strategies in the system. Redundancies (standby, backup, spare, alternative), maintenance activities (corrective, preventive, condition-based), and PHM strategies are some design approaches that have been deemed able to improve resilience in engineered systems [5]–[7]. Even so, less attention has been given by the design community to the study of how to regulate the response of a complex system *during* and/or after the occurrence of a failure event. Thus, the objective of this paper is to propose the use of control theory as a strategy to enable "real-time" resilient behavior in complex engineered systems.

Control theory in the engineering context is associated with how to govern the behavior of dynamical systems [8]. Key components involved in control theory are a reference signal, a controller, a system, and a control loop. A reference signal is an expected baseline performance signal. A controller is a mechanical, electrical, or computerized device. It can also be a control system, which consists of a collection of controllers. The main functions of a controller include monitoring the output signal, comparing the output signal to the reference signal, and adjusting the operating conditions of the system to bring the desired output closer to the reference signal. The system of interest is typically called the plant and is represented by either a transfer function or a state-space equation. A control system is designed as either an open loop or as a closed loop system. The difference between open loop and closed loop control is in their dependence on system output. The control action is independent of system output in open loop control, whereas the control action is dependent on system output in closed loop control. A closed loop control is also known as a feedback loop.

Control theory has been mainly employed by the control system engineering community to design advanced custom controllers. These controllers are equipped with the ability to do complex tasks required for the application of interest. Some examples of controllers and their system applications are cruise control in automobiles, autopilot in aircraft, temperature controller in heating/cooling systems, and acidity (pH) controller in water treatments. The advances in developing modern controllers can be found in, but are not limited to, adaptive controllers [9]–[11], resilient controllers [12], [13], optimal controllers [14], [15], robust controllers [16], [17], and combinations of the above, such as in the form of robust adaptive controllers [18], [19].

Control theory has various benefits in its application to an RCES, with the main advantage being its ability to regulate and govern system states, even *while* the failure is taking place. Thus, RP can be enabled and achieved in an RCES in a quicker and more efficient manner. Most of the complex engineered systems have a central controller to control the desired actions of the systems. Their control system can be either operated manually, automatically, or both. In the context of implementing control theory within an RCES, such a controller should be designed with the purpose of taking timely action to correct the shift in system performance in order to maintain an optimal performance level when a disturbance occurs.

Moreover, in designing an RCES, control theory can help system designers in evaluating how the system responds to a disruptive event and whether the resilience level designed into the complex systems is sufficient to counter against a particular failure. Resilience behavior of an RCES is attributed to the inherent ability to control the system in response to a disturbance, thereby maintaining a desired system performance level. Depending on the impact of the disturbance during and after the event, the design of the controller and the system can be adjusted to accommodate the changes. Thus, the system designers can decide on the best possible resilience design for developing new RCESs or retrofitting current RCESs.

The engineering resilience concept and control theory are fused in this paper to develop a resilience modeling and analysis methodology. The focus of this paper is directed toward enabling resilience behavior in RCESs through the control theory approach, instead of developing a resilient controller. The rest of this paper is organized as follows: Section II discusses resilience in engineering application in terms of attributes, performance curve, and metrics. Section III presents the developed general framework of modeling resilience based on control theory. A case study of resilience analysis for a power distribution system that focuses on transmission lines is presented in Section IV to demonstrate the effectiveness of the developed approach. Finally, conclusions are drawn in Section V, along with suggested future work.

II. Engineering Resilience

In an engineering context, resilience is often associated with the ability of the system to recover to its original system state postdisturbance [20], [21]. In this section, resilience attributes, its performance curves, and quantification metrics are discussed in relation to the system design perspective.

A. Resilience Attributes

Maximizing resilience could also be associated with minimizing vulnerability. In the reliability engineering context, it can be associated with minimizing the probability of failure [22]. Another essential feature of resilience behavior that sets resilience apart from other design concepts is the ability of the system to recover from failures or degraded performances [5], [23]. The recovery ability of an engineering system is another indicator of engineering resilience [22]. The basic resilience attributes in this paper are regarded as reliability and recovery. The whole resilience behavior in an RCES can thus be summarized as such: when the reliability of the system is insufficient, recovery will automatically take place. In other words, when failures are unavoidable, a system is said to be resilient if it possesses a failure recovery capability [23]–[25]. In addition to reliability and recovery, depending on the application of interest, there are other "ilities," for example, availability of resources, survivability of the system, or adaptability of the system to the failure, which are equally important and should be taken into account when analyzing resilience performance in an engineered system. Chalupnik *et al*. compared the "ilities" for system design protection against uncertainties [26].

It should be noted that in most RCESs, the resilience attributes do not occur naturally. The resilience attributes should be designed into the system in order for the system to possess some type of resilient behavior. Some of the examples can be seen through the application of incorporating redundancies in design, performing maintenance activities, and replacing defective components prior to system failures [5]. Improving system resiliency can be achieved through 1) improving the reliability of the system prior the occurrence of failures, and 2) enhancing the recovery ability of the system postfailure [20], [27]. A more advanced resilient system may possess other resilience attributes on top of reliability and recovery. Some examples are the ability of a system to monitor its own performance, forecast and respond to failures, and learn from failures [28].

B. Resilience Curves

In the presence of disruptive events, the system's resilience attributes take part in altering the system performance level, resulting in the distinguished system performance contours. These are known as the resilience curves. A typical resilience curve of an engineering system is portrayed in Fig. 1, where the system performance $P(t)$ is plotted against time t.

Typically, there are four common events that occur in the overall resilience scenario:

1) the reliability state, where the system operates under normal operating conditions with a system performance level P_o without failure. This state is also known as the reference state.
2) The unreliability state, or the vulnerable state. This occurs when the system reliability is not sufficient enough to absorb the impact of a disturbance event that occurs at time t_d. As a result, the system performance gradually decreases from P_o to the reduced performance level P_v.
3) The recovery state, where the system is being recovered back from the reduced P_v to the original P_o. This is the defining behavior of a resilient system, which can be achieved by altering the system states, if necessary, with the help of additional resources. The recovery period takes place from the time the system is in the lowest degraded states t_v to the time when the system is fully recovered t_n, or when the resources are exhausted during recovery. This period is also known as the control period [29].
3) The recovered steady state, where the system has been successfully recovered. The ideal case of resilience performance in the recovered steady state is indicated by a performance level matching that of the reliability state has been recovered. However, this scenario may not always be the case. Depending on how much the system can be recovered, the system could be restored to a higher or lower recovered steady state. An RCES is said to have a performance improvement if a higher recovered steady state was achieved, and said to deteriorate if a lower recovered steady state was obtained after recovery process when compared to performance level in the reliability state.

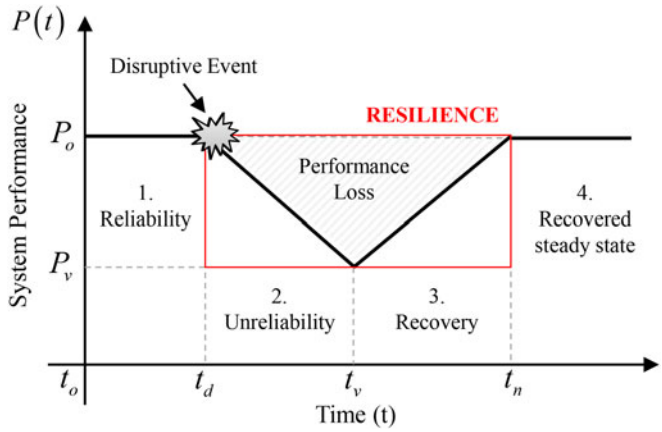

Fig. 1. Generic engineering resilience curve [30]–[32].

In the postoccurrence of the disruptive event, the degraded contour of the system performance portrayed in the vulnerability state may vary due to the severity of the disruptive events and how the system withstands the damage. The impact of the disruptions on the system can be captured by how fast the system performance degrades after the occurrence of disruptive events, as represented by the degree of vulnerability (θ) in Fig. 2. If the vulnerability curve exhibits a sharp drop, it can be said that the damaging impact of the disruptive event is so severe and fast that the system does not have enough time to resist the failures. Apart from the occurrence of disruptive events, the degraded contour of the system performance in the vulnerability state

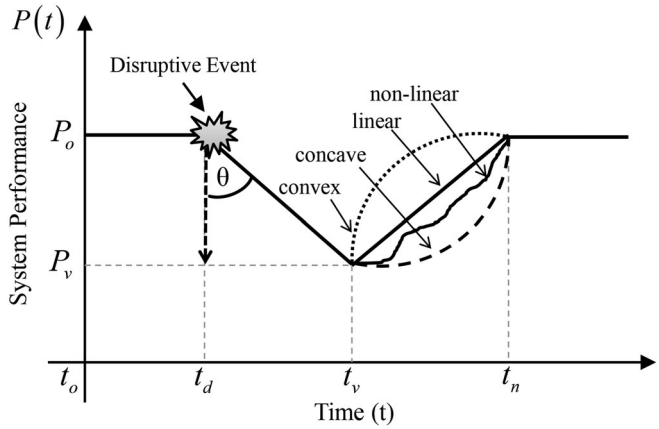

Fig. 2. Various contours in a general resilience curve [5], [33], [34].

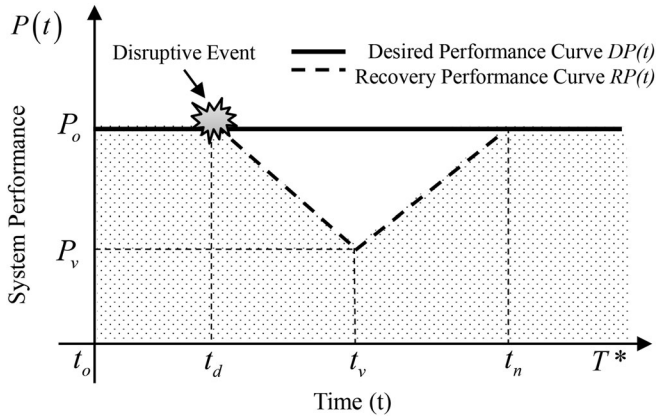

Fig. 3. Expected system performance curve versus recovery performance curve after a disruptive event.

could also happen due to system aging. Prolonged usage of the system minimizes the remaining useful life of the system and causes degraded system performance.

Similar to the degraded contour, the recovery contour of the system performance exhibits different profiles depending on the system's restorative capability, or how much resources are available to restore the system. There are cases where the recovered steady state could be higher or lower than the initial system performance level P_o. The ideal case for the recovered steady state is that the recovered system state is expected to be operating at the same performance level as the original system did without failures. In reality, contours are typically expected to show some degree of nonlinear behavior due to the presence of internal uncertainties in the system or external uncertainties from the surrounding operating environment. Regardless of the system performance profile in each stage of a resilience curve, a system is said to have a higher resilience if it exhibits lesser performance loss. The performance loss in the system is portrayed by the shaded triangle area in Fig. 1. Comparing the four recovery profiles (convex, concave, linear, and nonlinear) in Fig. 2, the preferred recovery profile is the convex topology. This is because a convex topology leads to a lower system performance loss when compared to the other recovery contours. Moreover, since the resilience scenario is time-dependent, the shorter the recovery period, from t_v to t_n, the higher the level of resilience in the system.

C. Resilience Metric

The evaluation of the resilience level designed into RCES with multidimensional performance requirements can be challenging. There are many resilience quantification metrics that have been previously proposed by various researchers in diverse engineering applications [5]. In this paper, the resilience level in RCES is calculated based on the overall system performance instead of evaluating the RP of each component within the RCES. The desired curve expresses how the system is expected to perform in the reliability state without any failures and the resilience curve contains the information on how the RCES behaves when subjected to disruptive events. Both the desired curve and resilience curve are depicted in Fig. 3.

Once the recovery actions have been completed postdisruption, a complete four-stage resilience curve can be obtained. Furthermore, the resilience level possessed by the RCES can be measured by comparing the area under its system performance recovery curve RP(t) with the area under its DP curve DP(t) [5], [35]. The area under the curve can be calculated by taking the integral value during the period of the resilience scenario, from t_o to T^*. Mathematically, the resilience level in RCES can be obtained by

$$\Psi = \frac{\int_{t_o}^{T^*} \mathrm{RP}\,(t)\,dt}{\int_{t_o}^{T^*} \mathrm{DP}\,(t)\,dt} \tag{1}$$

where Ψ is the system resilience level, t_o is the initial scenario time, and T^* is an extended time period that is enough to capture the overall scenario of interest. Moreover, RP(t) indicates the recovery of system performance at time t after the occurrence of a disruptive event, which characterizes the system response in the presence of a disruptive event from time t_o to T^*, and DP(t) is the DP at time t that characterizes the system performance if no disruptions occur from time t_o to T^* In Fig. 3, the DP curve is portrayed in a straight line, whereas in reality the DP(t) is most likely to follow a nonlinear function.

III. General Framework of Modeling Resilience Based on Control Theory

To enable resilience behavior in RCES, the concept of fusing control theory and engineering resilience is introduced. First, the selection of controller and the representation of the system are discussed. The general modeling framework through the utilization of control theory is then presented as an approach to enable resilient behavior and measure the resiliency level in an RCES.

A. Control Theory

There are four key components in a control system. These are a reference signal, a controller, a system, and a control or feedback loop. A generic closed-loop control theory concept is illustrated in Fig. 4. A reference signal is a baseline signal in

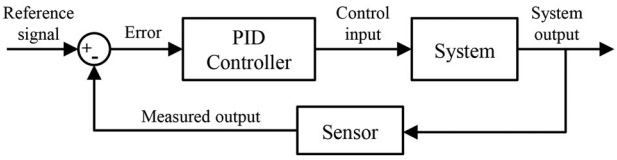

Fig. 4. Typical control theory block diagram.

which the desired system output is expected to follow. The step function, sine/cosine functions, and other linear or nonlinear functions are often used to define reference signals. In addition, reference signals can be obtained experimentally or based on historical data. The difference between the reference signal minus the measured output signal is the error signal *e*(*t*).

Adjusting signal inputs to the system is one key function of a controller. There are many types of advanced controllers that have been developed by researchers in the controls community. However, since the focus of this paper is not directed toward the advancement of existing controllers, a commonly used PID controller is employed in this paper. A PID controller, which relies on the measured output variable, has been known for its simplicity and efficiency in solving many real-world control applications [36].

A PID controller has a closed-loop feedback control mechanism. Thus, it can be utilized to continuously calculate the error value *e*(*t*) which is the discrepancy between the measured output signal and the reference signal. Three main components of a PID controller are

1) the *proportional term*, which accounts for the present error *e*(*t*). The proportional response can be calculated by multiplying the current error with a proportional gain constant of K_p.
2) the *integral term*, which accounts for the past error. The past error is the sum of the instantaneous error signal from $t = 0$ up to the instant time *t*, which should have been amended previously. The integral response can be obtained by multiplying the accumulated error with an integral gain constant of K_i.
3) the *derivative term*, which accounts for the possible future error. The derivative term can be adjusted by multiplying the rate of change of the error with a derivative gain constant K_d [36].

In a time domain, the output of a PID controller is represented by the adjusted control variables *u*(*t*) in terms of the error signal *e*(*t*), which can be mathematically expressed as

$$u(t) = \underbrace{K_p e(t)}_{\text{Proportional}} + \underbrace{K_i \int_0^t e(\tau)\, d\tau}_{\text{Integral}} + \underbrace{K_d \frac{d}{dt} e(t)}_{\text{Derivative}} \tag{2}$$

where τ is the integration variable representing time, which takes the values from time $t = 0$ to the present time *t*. If a frequency domain is more preferable, the transfer function can be employed. The transfer function *G*(*s*) of a PID controller is generally written as

$$G(s) = K_p + K_i \frac{1}{s} + K_d s \tag{3}$$

TABLE I
EFFECTS OF INCREASING PID GAINS INDEPENDENTLY [36]

Parameter	Rise Time	Overshoot	Settling Time	Steady-State Error	Stability
K_p	Decrease	Increase	Small Increase	Decrease	Degrade
K_i	Decrease	Increase	Increase	Large Decrease	Degrade
K_d	Small Decrease	Decrease	Decrease	Minor change	Improve

where *s* is the complex signal. The gains in a PID controller (K_p, K_i, and K_d) are non-negative values. Their value can be tuned as desired to represent the ability of the controller to perform correction in minimizing the error values for specific system requirements. The effect of increasing each of the PID controller gains independently on the system dynamics in a closed-loop response is summarized in Table I.

Rise time is the time it takes for the system output to rise beyond the desired level for the first time when trying to minimize the error. Overshoot is the difference between the peak level and the steady state level of the system. Settling time is the time it takes for the system to converge to its steady state. Steady state error is the difference between the system steady state output and desired output or the reference signal. Stability defines whether the system steady state converges to the desired output, fluctuates around it, or diverges from it.

In the context of governing the system to achieve resilience, a well-tuned PID controller is able to provide the system with a better stability during control process. The proportional gain K_p and the integral gain K_i describe the speed of change in the output. The higher the K_p and/or K_i value, the faster the output will be adjusted. The difference in K_p and K_i is that K_p alters the output based on the information of current errors, whereas K_i corrects error according to the accumulated past errors. The derivative K_d gain has an effect on increasing the stability and transient response. However, K_d has an opposite effect with K_p and K_i; it slows down the change of rate in the output. These three constants should be tuned before the controller can be employed to realize resiliency in the system by optimally controlling the system variables to match the DP.

There are two general ways to represent a system, state-space equations, and transfer functions. For many physical systems, their dynamic behavior can be modeled as a set of first-order differential equations:

$$\dot{x} = \frac{dx}{dt} = f(x(t), u(t), t) \tag{4}$$

where *x*(*t*) is a set of variables representing system states at time *t*, and *u*(*t*) is control input vector to the system at time *t*. The dynamics of many physical systems can be approximated as linear; given that each state variable remains within a sufficiently small operating range about the point of linearization [37]. The standard state-space function of a continuous linear

time-varying system is given by

$$\text{Input } \dot{x}(t) = A(t)x(t) + B(t)u(t) \tag{5}$$

$$\text{Output } y(t) = C(t)x(t) + D(t)u(t) \tag{6}$$

where $\dot{x}(t)$ is the time derivative of the state vector x, $A(t)$ is the system matrix at time t, $x(t)$ is the system state vector at time t, $B(t)$ is the control input matrix at time t, $u(t)$ is the control input vector at time t, $y(t)$ is the output vector at time t, $C(t)$ is the output matrix at time t, and $D(t)$ is the feedforward matrix at time t. In some cases, if the model does not have a feedforward matrix, $D(t)$ is equal to zero.

Another system representation is the transfer function, which describes a system based on its inputs and outputs. A closed loop system transfer function $G(s)$ is represented as the ratio of the output of the system $Y(s)$ to its input $U(s)$, where s is a complex signal:

$$G(s) = \frac{Y(s)}{U(s)}. \tag{7}$$

Both system state and transfer function are commonly used in representing a system. The state-space equations represent a system in the time domain, and the transfer functions represent a system in the frequency domain. Time domain can be converted to frequency domain via Laplace transform, and frequency domain can be converted to time domain via inverse Laplace. Depending on which domain is of the particular interest, system state-space equations can be converted to transfer functions, and vice versa.

Most electrical systems can be represented as an *RLC* circuit, which is a simple series combination of three electrical elements: a resistor (R), an inductor (L), and a capacitor (C). To demonstrate how state-space models from a physical system are obtained, an example of an *RLC* circuit is presented (see Fig. 5).

Consider the circuit driven by a voltage source $V(t)$, which is also considered as the input to the system. The state variables of interest are the charge in the capacitor $Q(t)$ and the current around the circuit $I(t)$ at time t. From Kirchhoff's Law, which states that the sum of voltage around the closed loop circuit is zero, the governing equation is given as

$$\begin{aligned} &V(t) - V_R(t) - V_L(t) - V_C(t) = 0 \\ &V(t) - I(t)R - L\dot{I}(t) - \frac{Q(t)}{C} = 0 \\ &I(t) = \dot{Q}(t) \qquad \dot{I}(t) = \frac{dI}{dt} \quad Q(t) = \int I\, dt \end{aligned} \tag{8}$$

where $V_R(t)$, $V_L(t)$, and $V_C(t)$ is the voltage across the resistor, inductor, and capacitor at time t, respectively.

The system state-space representation can be determined by choosing the state-space variables x. If $x_1 = Q(t)$ and $x_2 = I(t)$ are the selected state variables, the dynamic behavior of the *RLC* circuit can be derived from a set of first-order differential equations, given by

$$\dot{x} = \begin{bmatrix} \dot{x}_1 \\ \dot{x}_2 \end{bmatrix} = \begin{bmatrix} I(t) \\ dI/dt \end{bmatrix} = \begin{bmatrix} 0 & 1 \\ -R/L & -1/LC \end{bmatrix} \begin{bmatrix} x_1 \\ x_2 \end{bmatrix} + \begin{bmatrix} 0 \\ 1/L \end{bmatrix} V(t). \tag{9}$$

For example, if we are interested in controlling the current $I(t)$, the output equation y can be rewritten as

$$y(t) = C(t)x(t) + 0 = \begin{bmatrix} 0 & 1 \end{bmatrix} \begin{bmatrix} Q(t) \\ I(t) \end{bmatrix}. \tag{10}$$

More information on other ways of deriving a state-space model of an *RLC* circuit can be found in [38]–[40]. According to Section 19 of the *Standard Handbook of Electronic Engineering* [40], in control systems, the state variables x can represent physical quantities that may be measured, such as voltage and current; or they can be in the form of mathematical quantities which may or may not have direct physical interpretation in the system. This is another advantage of control theory, since system parameters that may be hard to obtain or directly measure can be incorporated in the modeling process of evaluating resilience scenarios in RCESs.

B. Modeling Resilience Concept Based on Control Theory

Prior to developing a new RCES or retrofitting old ones, system designers have to determine if the resilience capability designed into the system is sufficient. This stage of design typically involves extensive modeling efforts. The essential modeling elements required to simulate a resilient scenario with the objective of analyzing the resilient behavior of a system against a certain disturbance are

1) the *degraded states* of the system to simulate the impact of disruptive events on the system and to study the reliability of the system to withstand disruptions,
2) the *recovery strategies* to simulate the capability of the system to restore itself from the degraded state with or without assistance, and
3) the *DP* to analyze the resiliency level of the system, which can be determined by comparing the recovered system performance to the initial performance.

By employing control theory, the reference signal can be viewed as the DP or the initial reliable performance. The controller is tasked with the objective of correcting errors to bring the output signal closer to the reference signal, which can be analogized as a restoration strategy. The initial state and disrupted state of the system can be represented as two different system state-space functions. Different types of disruptive events that cause various impacts on system performance can be represented by different state-space functions as well. Any changes in the system characteristics will affect the state-space function of the system.

Fig. 6 shows the modeling elements of the resilience concept within the context of a control system. As discussed previously, there is two general way to represent a system, state-space

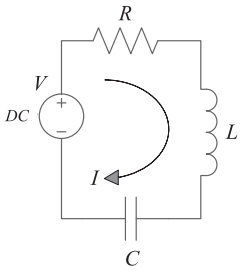

Fig. 5. A typical *RLC* circuit.

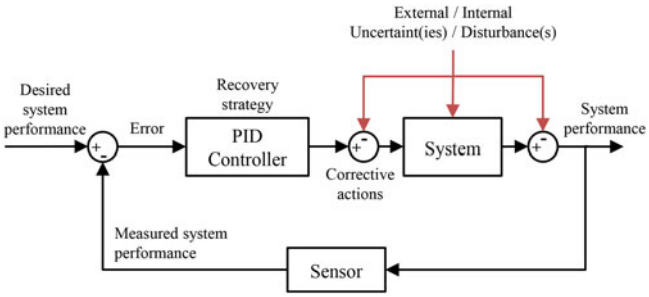

Fig. 6. Resilience concept viewed in the control block diagram.

equations, and transfer functions depending on the domain of interest is time or frequency. This paper is more interested in the time domain; thus, system state-space representation was employed instead of the transfer function.

External and internal disturbance conditions can be incorporated to simulate the degraded performance of the system. The impact of external disturbances can be subtracted from the corrective actions signal and/or the system output signal since these types of disturbances are considered to occur outside the system state (prior to the system input or at the system output). On the other hand, internal disturbances and uncertainties are deemed to have an effect on the characteristics of the system. Thus, the state-space model or transfer function of the system may change when internal disturbances are present.

If there are sufficient resilience abilities designed in the system, the performance output of the system (with the help of corrective action from the controller) is expected to portray the behavior shown in Fig. 7. When there is degraded performance detected in the system, the controller should simultaneously be able to take timely action to correct the discrepancies between the DP and the output performance. To achieve this, the PID controller can be tuned as desired through the value of the gains K_p, K_i, and K_d. More advanced types of controllers (optimal, adaptive, etc.) may also be used to achieve this goal.

Note that converting the performance index of general engineered systems into the control system is one of the key steps for the application of the presented resilience by a control framework. In the literature, several resilience metrics have been developed [5], which can be used to convert general system performance index into one of those resilience metrics. As a representative, the resilience metric developed in [3] considers two essential attributes of the system performance, the reliability and the restoration, which can be obtained based on the system performance in a probabilistic manner using advanced

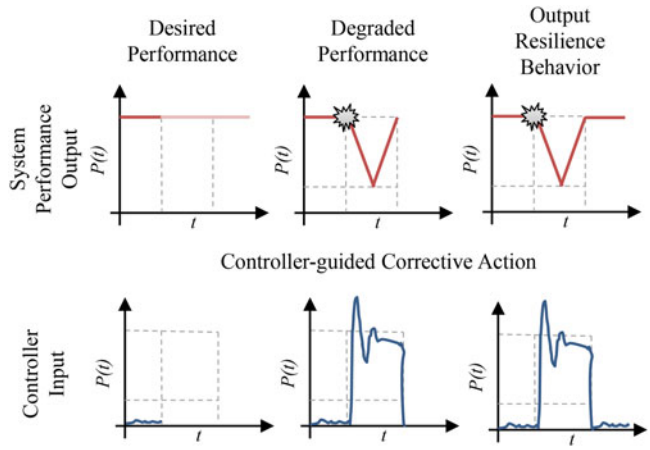

Fig. 7. Resilience behavior as a result of corrective action from the controller.

system modeling tools such as the Bayesian network or dynamic Bayesian network [3]. In the case of dynamic systems with implicit state representations, the self-cognizant dynamic system approach [41], [42] can also be conveniently used for system performance prediction and converting general engineered systems into control systems.

IV. Case Study

Power regulation over the years has been studied tremendously due to its complexity in dividing and supplying power from different sources to various sectors of energy customers while meeting the electricity demands at every instantaneous time. In this case study, the resilience of a local electricity transmission system was studied. The current transmission system was proposed to be retrofitted with a clean energy transmission system. The proposed approach of employing control theory will be applied to study the resilience scenario in the future retrofitted system. In this section, the description of the case study will first be detailed, followed by the modeling approach, results, and discussion.

A. Case Study Description

Renewable energy has gained attention over the past years as a promising candidate for a low-cost clean energy solution. However, renewable energy is considered as intermittent energy since it is not continuously available at any given time due to factors beyond direct operational controls. Renewable energy is highly depending on weather conditions, resulting in high-variation and inconsistent daily energy generation. In some days, where weather conditions are not suitable, no energy can be generated. Thus, current utility companies and customers still have to depend on nonrenewable energy sources, such as coal-fired power plants, to deliver stable, reliable, and affordable electricity.

On days when weather conditions are conducive to generating electricity, a substantial amount of affordable and clean electricity can be generated. During these days, to effectively and efficiently incorporate this electricity into the power grid, power regulators usually attempt to displace nonrenewable energy with

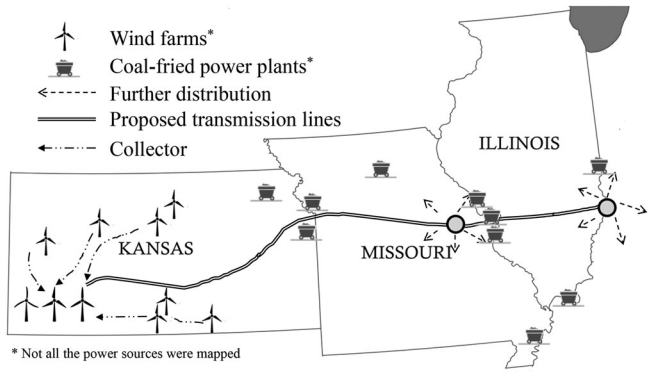

Fig. 8. Transmission line from the State of Kansas in the United States.

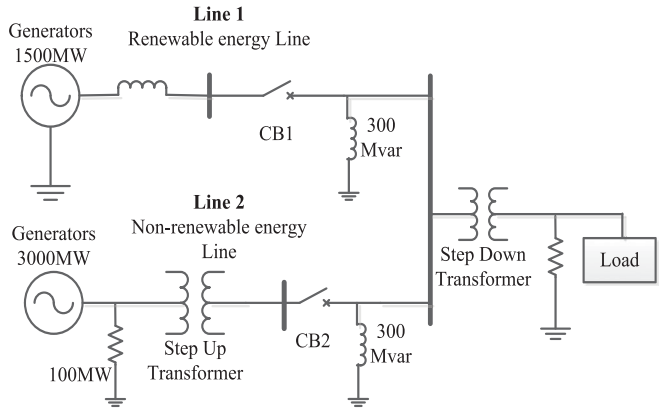

Fig. 9. Electrical circuit consisting of two transmission lines.

renewable energy. Furthermore, after satisfying nominal electrical demands, this excess renewable energy that has already been generated will be wasted due to limitations in power storage capability. While much research has been directed toward developing advanced battery energy storage systems to store such excess energy, another approach to effectively utilize the excess renewable energy is to supply it to other further regions that do not have access to renewable energy. Thus, more electricity demands can be fulfilled with the renewable energy instead of the nonrenewable energy.

The state of Kansas in the United States is known for its high potential capacity for wind power as one source of renewable energy. However, one of the challenges faced by many wind farms in Kansas is that there is a significant amount of renewable energy excess that has been wasted over the years due to excessive generation during high-season and inadequate power grid regulation. One of the solutions proposed by the local utility companies is to collect and sell the excess energy to other areas that do not have access to renewable energy. A recent project has been proposed to develop a renewable energy collector center and clean energy transmission lines from the state of Kansas to the neighboring states (see Fig. 8). The excess energy from multiple wind farms in Kansas will be collected at a central collector. The excess energy will be further distributed through the clean energy transmission lines to the neighboring states. The objective of this case study is to evaluate the resiliency of the electrical distribution system when the new transmission lines are retrofitted in place of the current transmission lines.

For the current system, the disturbances based on the historical data of occurrences can be categorized as internal and external disturbances. Internal disturbances have typically included component failures and short circuits, whereas external disturbances were typically induced by nature, such as tornados, thunderstorm, and high winds, which may threaten to cut power transmission lines. The severity of both disturbances was measured in terms of power loss during a period of time. Moreover, inherent uncertainties at every instantaneous time were taken into consideration while modeling the system to account for noise that exists during actual operating conditions. The presented case study was carried out within the MATLAB/Simulink environment.

B. Modeling

The existing transmission lines are planned to be retrofitted by incorporating the clean energy transmission lines. The project proposal proposed the development of a 700-mile major clean transmission line, which is planned to be divided into two sections of a 500-mile line and a 200-mile line. The physical power system retrofit can be represented as an equivalent electrical circuit in Fig. 9, showing both renewable and nonrenewable transmission lines serving energy to two regions, represented as a combined load. The resilience scenario was conducted on a daily basis, or in other words, on a 24-h timescale.

Data employed for this case study were provided by the project sponsors, a local utility company. All data were assumed to have gone through a learning and validation process. Moreover, the components and other relevant historical data had been appropriately scaled to maintain project confidentiality.

The desired system performance, which acted as the reference signals, was studied based on the ability of the transmission system to output daily power required to fulfill the demand. The total daily demand was computed as the total average usage of electricity in residential, commercial, and industrial sectors in a region over the past year. The historical data of daily demand were found to mimic a sine function, and thus an adjusted sine wave was used as the reference signal in the model. The highest demand was set to be 50 MWh at around 4–6 P.M. or the 16–18th time step in the model.

The default Simulink PID controller block was employed as the controller in the case study. The PID controller was tuned periodically to provide a swift response to different types of disruptions. This is reasoned with the claim where a system is resilient to different disruptions.

The external disturbances were considered to affect the control input to the system and/or the output of the system. Since the external disturbances were unpredictable in most cases, the behavior of the external disturbances was modeled as a step function where at the time of occurrence, the damage done to the system could be simultaneously applied as a sharp drop in system performance. The external disturbances were applied over a certain period of time from $t = 0$ to 10, with a major damage occurring at $t = 10$. During $t = 0$–10, a constant 5 MW

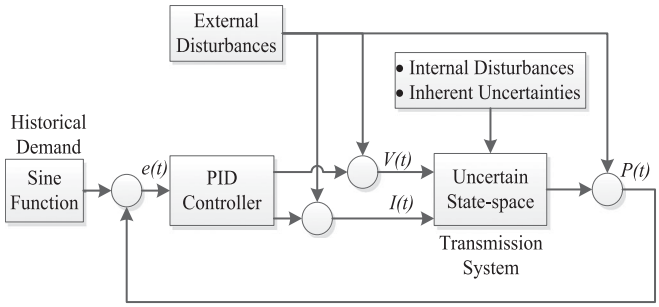

Fig. 10. Schematic control architecture modeled in MATLAB/Simulink.

drop was applied to the system to mimic the prolonged external disturbances such as the disasters induced by nature. The total damage done to the system was presented with an additional 5 MW drop by the end of the external disturbances, totaling a 10 MW drop at $t = 10$.

Component failures and operator error are deemed as internal disturbances. The total damage due to internal disturbances resulted in a lower power output. The internal disturbances were represented through various failed state-space models corresponding to a 10–30% power loss range. The internal disturbances were set to happen at time $t = 10$.

Gaussian noise has been added to the state-space model of the system to represent the inherent uncertainties in the system. These inherent uncertainties may result in variations or instability in the performance output, which can be considered as a type of inherent disturbance.

The state-space functions of the presented case study were obtained by converting the system to an *RLC* circuit as presented in the previous section. Furthermore, the equivalent circuit models were validated through modeling in the MATLAB Simscape Power Systems toolbox. The state variables were current $I(t)$ and voltage $V(t)$, and the output of interest was the system performance in terms of power output $P(t)$. The simulation time period was set to be daily or 24-time steps in Simulink. The simplified MATLAB/Simulink model employing the control theory as the proposed approach to enable resilience behavior in a system is shown in Fig. 10.

Different combinations among external, internal, and inherent disturbances were simulated. The resulting resilience curves for each disturbance scenario were further employed to quantify the resilience level of the system when subjected to a particular disturbance. The resilience level was quantified based on (1), where the resilience level is defined as the ratio of the area under the RP curve over the DP curve during the resilience scenario from $t = 0$ to 24. Another method to identify if the system is resilient against a particular disturbance is through the analysis of the convergence capability of the resulting resilience curve.

C. Results and Discussion

The simulation results for three different disruption scenarios are tabulated in Table II. The external disruption represents an episode of a longer duration disturbance that occurred at time $t = 0$–10. The internal disturbance corresponds to component

TABLE II
RESILIENCE LEVEL AND CONVERGENCES FOR DIFFERENT DISRUPTIONS

Scenario	Disturbances			Ψ (%)	Convergence
	External	Internal	Inherent		
1.		No failure		99.6	Yes
2.	•			87.0	Yes
3.		•		92.5	Yes
4.	•	•		79.4	No
5.			•	99.5	Yes
6.	•		•	85.7	Yes
7.		•	•	91.3	Yes
8.	•	•	•	78.6	No

failures or operating errors resulting in a 10% power output loss. The inherent disturbance expresses the operational variations exhibited in the system. Eight scenarios were presented. In scenarios 1–4, the system's inherent uncertainties are not included in the resilience assessment. The inherent uncertainties are featured in scenarios 5 and 6.

The resilience level for each scenario was presented as a percentage value. The ideal or baseline condition is when there is no loss of system performance observed or when the system is operating as desired (scenario 1). Since resilience is quantified as a ratio obtained by comparing the resilience curves to the desired curves, under the ideal condition, the system is indicated by a resilience value of 100% or $\Psi = 1$. On the other hand, if there is any loss of performance due to any type of disturbance, the resilience value was observed to be less than 100%. For example, in scenario 2, where the system was subjected to the occurrence of external disturbances, the resilience level was found to be 87%. This means that in the presence of external failures, the transmission system has a success rate of 87% of recovering the DP over a 24 h period of time. Since the DP was taken as the historical demand, it also means that the transmission system was expected to be able to fulfill 87% of the daily electricity demand although external failures were present.

From Table II, external disturbances were found to damage the system more than internal disturbances. This is shown by the lower resilience levels found in scenario 2 compared with scenario 3, or scenario 6 compared with scenario 7. In other words, higher resilience levels were observed for the system in the presence of internal disturbances compared to external disturbances. Thus, it can be further concluded that the transmission system in this case study was found to be more resilient against internal failures compared to external failures.

As has been noted previously, a system has different resiliency levels toward different types and intensities of disruptive events. To justify whether the resilience level in the system was sufficiently designed into the system, a resilience threshold value was set against various disturbances. A threshold of resilience level in this case study was selected to be 85%, which means that the system of interest should be able to fulfill at least 85% of the daily electricity demand or should not exceed more than 15% of daily power loss when the system was disrupted in any manner. With the 85% resilience threshold, the resilience level designed in the system was found to be insufficient to protect

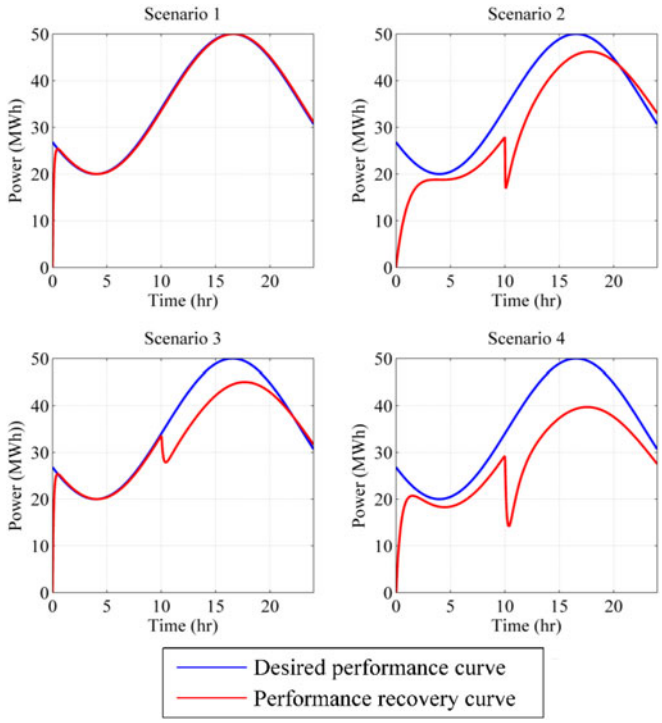

Fig. 11. System performance curves without inherent uncertainties.

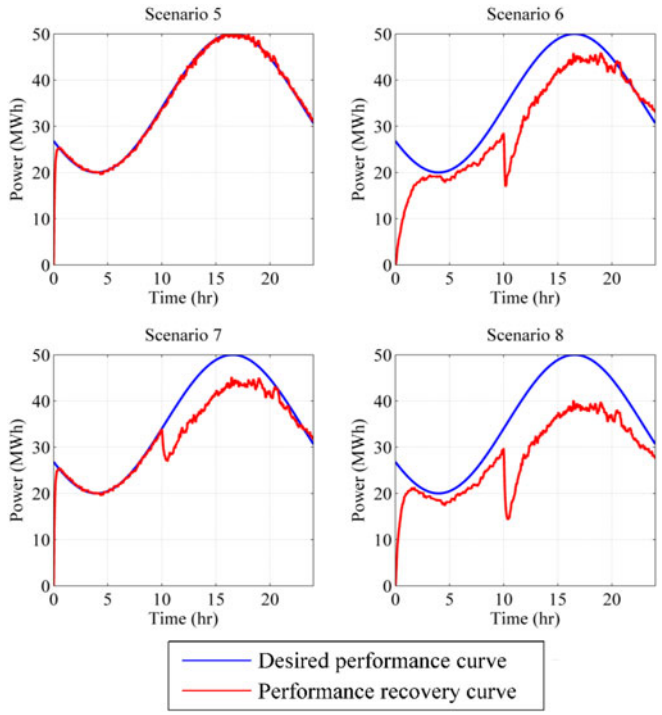

Fig. 12. System performance curves featuring inherent uncertainties.

the system against disturbances induced by the combination of both external and internal factors (scenarios 4 and 8).

The corresponding resilience curves obtained for each scenario are portrayed in Fig. 11 for scenarios 1–4 (without inherent uncertainties) and Fig. 12 for scenarios 5–8 (with inherent uncertainties). The resilience level for the scenarios with inherent uncertainties in the system was found to yield a slightly lower value when compared to the scenarios without inherent uncertainties (see Table II). Thus, estimating resilience with linear curves instead of nonlinear curves could be deemed as overestimating the resilience capability in the system.

Another way to identify the resiliency of the system over a period of time is by comparing the convergences of the RP curve with the DP curve. The system is said to converge if the system is able to successfully catch up with the DP curve from its degraded states within a specific recovery period. The end of the recovery period, in this case, is at the end of a day, or $t = 24$.

In all the scenarios, except for scenarios 4 and 8, the system was found to be able to converge. In some cases where there were discrepancies found in the end result of the daily electricity demand and the DP, such as in scenarios 2 and 4, the system was still deemed to converge. This is because, after the disruptions, the controller was able to help the system recover from its degraded state and meet the DP at some point before the end of the specified recovery period. In scenarios 4 and 8, where the system was subjected to the combinations of internal and external failures, the system was not able to converge. Although scenario 4 and scenario 8 were not able to recover by the end of $t = 24$, both scenarios should be able to converge if they are given an adequate length of the recovery period.

The convergence behavior was found to correspond to the analysis based on the resilience level where the resilience level designed into the system was insufficient when the system is subjected to the collateral damage induced by both internal and external failures (scenarios 4 and 8). Some of the suspected reasons for not converging are

1) the combined failures are too severe for the controller to correct or the system to respond to,
2) the PID controller is insufficient to keep up with the failures, and
3) the system is not resilient against those particular failures. Thus, improvement strategies to improve resilience against the combination of both external and internal disturbances can be directed toward improving the system as well as the controller.

The PID controller employed in the case study plays a major role in mitigating failures and assisting the recovery process. All the eight scenarios presented in Table I were performed with the same PID controller settings of $K_p = 10$, $K_i = 100$, and $K_d = -0.2$. Without changing the PID controller setting, Fig. 13 shows various resilience curves obtained for scenario 3 where the system was subjected to the power output loss ranging from 10% to 30% due to the internal disturbances. It can be seen that with power output loss beyond 10%, the system could not be recovered in the same day. One of the reasons is with the same PID controller settings; the PID controller was lacking in handling more severe failure impacts. The controller should, thus, be adjusted or enhanced to accommodate different levels of failure impact. So that, when the system is subjected to more a severe performance degradation, the controller is able to provide a faster response in mitigating failures.

The impact of tuning the gains (K_p, K_i, and K_d) in the PID controller employed in this case study was also studied. It was

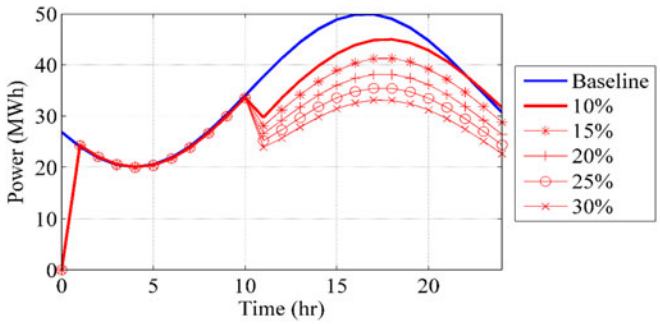

Fig. 13. Scenario 3 with various damage impacts.

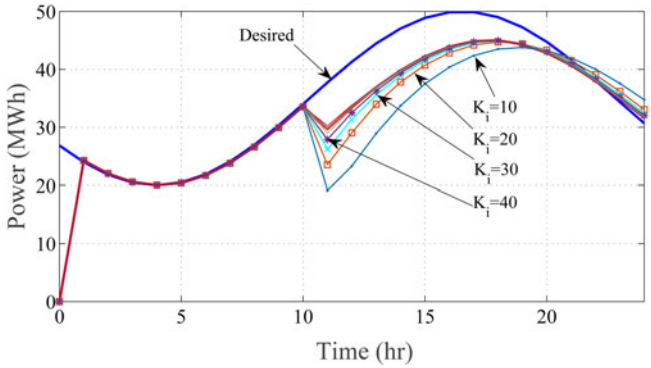

Fig. 14. Effect of tuning K_i in scenario 3.

found that tuning the proportional gain K_p and the derivative gain K_d in this case study did not show any significant difference in mitigating failures and recovering the system from degraded states. However, the major controller behavior was found to be attributed from the integral gain K_i. Fig. 14 portrays the behavior of the controller with different K_i setting in scenario 3 where the system suffered from 10% power loss due to the presence of internal disturbances. It can be seen that the controller response faster by increasing its K_i setting. In addition, the controller performance was also found to be stabilized at higher K_i. This could be further interpreted that controllers also possess a maximum capability threshold. Thus, further advancements in controller capability should be incorporated to ensure a more resilient system.

In the concurrent development of resilience functions in complex engineered systems under uncertainty, the resilience concept and control theory concept are found to complement each other. The engineering resilient concept promotes failure recovery in the presence of disruptive events, whereas control theory employs a controller to regulate system states to bring the system output closer to the DP—in other words, to enable resilient behavior in the system.

Control theory has various benefits in application to a resilient engineered system. The main advantage is its ability to regulate, govern, and modify system states through a controller. As seen in the presented case study, in scenarios 2, 3, 6, and 7, the discrepancies between the desired and output performance were corrected by the PID controller while the failure was taking place. A controller in the engineering resilience context can, thus, be considered as a failure recovery strategy, where during the presence of failures, the system performance is simultaneously maintained by the controller so that it does not degrade further. In addition to maintaining system performance during its degraded states, the controller also aided in improving the system performance corresponding to the DP.

In the physical context of implementing control theory within a complex engineered system, resilient behavior can be enabled by integrating a controller into the system. Such a controller should be designed in a way such that, when a disturbance is occurring, the controller should simultaneously be able to take timely action to correct the shift in system performance. Since the focus of this study is to bridge control theory and the engineering resilience concept, the focus has not been on to the design of the controller itself, but on the potential for controllers to act as resilience-enablers. As shown in Fig. 13, the PID controller used in the case study has limitations on its ability to correct the system. Given that the PID controller employed in the case study is only intended to demonstrate the proposed approach, a more advanced control mechanism should be sought for the applications in the real complex engineered systems in the future. It is true that the parameters for system control such as the PID controller used in the case study should be related to real design factors to show the resilience impact. As this paper primarily introduces the system resilience as a postdisruption control problem, thus a PID controller with simple parameter settings has been used to demonstrate the concept whereas the control design factors have been omitted.

Moreover, in the presented case study, internal and external failures were only subjected to the system or the outcome of the system, and the controller was assumed to be free from these failures. In reality, controllers are not immune to failures and are themselves required to be resilient against failures. Thus, as a direction of future work, collaborations with control system engineers will be established to develop a more advanced and resilient controller suited for this application of interest.

One of the bigger challenges faced in studying complex engineered systems is to take into account all parameters or state variables into the modeling process. Some of these important state variables are not easily obtained or measured in reality. In control theory, the state variables of the system can be approximated through mathematical formulations and further converted to the physical context. In the early design stage, this feature of control theory can be very accommodating to the system designers in finding the right system parameters for the DP output. Thus, the physical design of the system can be modified during the design stage. In addition, the resilience level of the system against a particular failure can be measured further once the resilient behavior of the system toward a particular failure mode is made known to system designers. In the situation where there are no mathematical or state-space equations available to estimate the true system, the commonly employed method is decomposition. However, decomposing a complex system may not necessarily represent the true complex system since there may be some parameters/variables that are either simplified or omitted. To overcome this challenge, a future study of this work will be directed toward learning the complex system to

obtain the mathematical equations to represent the true complex system.

The resilience threshold introduced in the case study may not be optimal for all engineered systems, especially in those extremely crucial systems where failures cannot be afforded. In this type of system, the threshold for the resilience level should be set higher to accommodate for minimum performance loss or faster recovery evaluation. Additionally, improving the resilience level in a system is always associated with an additional cost. When it comes to a design decision to ensure a sufficient level of resilience in a system, the cost factor should be simultaneously considered to also ensure affordability. Cost factors can be incurred in both advanced controllers and the system itself. The resilience level could be improved in the system design by incorporating more redundancies in the system design as one example, or by selecting a proper controller to control the system. This research could also be leveraged to involve a cost-benefit assessment associated with the different design alternatives considering interdependencies or the controller selection.

V. Conclusion

This paper presented a control theory based resilience modeling and analysis approach to enable a failure recovery scheme in the design of RCESs. The desired system performance was modeled as a reference signal, a recovery scheme was enabled by employing a control mechanism of the system, and further, the dynamics of the system was represented by different state-space models. Three types of disturbance and uncertainties were studied in the case study: external, internal, and inherent. The results showed that by employing the appropriate control, the system performance could be restored in a specific period in most of the presented failure scenarios. Further advancements in the control mechanisms for complex engineered systems could be sought to obtain a better control over the system against more adverse failures. Apart from fusing the engineering resilience concept with control theory, the presented study also expects to aid in the development of RCESs and/or retrofitting the current complex engineered systems to be resilient against certain failures.

References

[1] J. M. Ottino, "Engineering complex systems," *Nature*, vol. 427, no. 6973, 2004, Art. no. 399.

[2] E. Zio and G. Sansavini, "Modeling interdependent network systems for identifying cascade-safe operating margins," *IEEE Trans. Rel.*, vol. 60, no. 1, pp. 94–101, Mar. 2011.

[3] N. Yodo and P. Wang, "Resilience modeling and quantification for engineered systems using Bayesian networks," *J. Mech. Des.*, vol. 138, no. 3, 2016, Art. no. 031404.

[4] S. A. Rinaldi, J. P. Peerenboom, and T. K. Kelly, "Identifying, understanding, and analyzing critical infrastructure interdependencies," *IEEE Control Syst. Mag.*, vol. 21, no. 6, pp. 11–25, Dec. 2001.

[5] N. Yodo and P. Wang, "Engineering resilience quantification and system design implications: A literature survey," *J. Mech. Des.*, vol. 138, no. 11, 2016, Art. no. 111408.

[6] M. Marseguerra *et al.*, "Optimal design of reliable network systems in presence of uncertainty," *IEEE Trans. Rel.*, vol. 54, no. 2, pp. 243–253, Jun. 2005.

[7] M. Compare and E. Zio, "Predictive maintenance by risk sensitive particle filtering," *IEEE Trans. Rel.*, vol. 63, no. 1, pp. 134–143, Mar. 2014.

[8] S. Simrock, "Control theory," in *Proc. CERN Accelerator School Digital Signal Process.*, 2007, pp. 73–130.

[9] M. Rafi and J. Steck, "Response and recovery of an MRAC advanced flight control system to wake vortex encounters," in *Proc. AIAA Infotech@ Aerosp. Conf.*, Boston, MA, USA, Aug. 2013, Paper AIAA 2013-5209.

[10] M. Rafi, J. E. Steck, and J. Watkins, "Application of a Kalman filter for reduction of sensor/turbulence-induced noise within a model reference adaptive controller," in *Proc. AIAA Guid., Navig., Control Conf.*, 2016, Paper AIAA 2016-1625.

[11] M. Rafi, J. Steck, and K. Rokhsaz, "A microburst response and recovery scheme using advanced flight envelope protection," in *Proc. AIAA Guid., Navig., Control Conf. Exhib.*, Minneapolis, MN, USA, 2012, Paper AIAA 2012-4444.

[12] D. Hock *et al.*, "Pareto-optimal resilient controller placement in SDN-based core networks," in *Proc. 2013 25th Int. Teletraffic Congr.*, 2013, pp. 1–9.

[13] M. Arruda and D. Steck, "Dynamic inverse resilient control of a damaged asymmetric general aviation aircraft," in *Proc. 48th AIAA Aerosp. Sci. Meeting Including New Horizons Forum Aerosp. Expo.*, 2010, Paper AIAA 2010-946.

[14] W. Nobleheart, A. Chakravarthy, and N. Nguyen, "Optimal and decentralized controller designs for an elastically shaped aircraft," in *Proc. 55th AIAA/ASMe/ASCE/AHS/SC Struct., Struct. Dyn. Mater. Conf.*, 2014, Paper AIAA 2014-1042.

[15] A. Bitoleanu, M. Popescu, and V. Suru, "Optimal controllers design in indirect current control system of active dc-traction substation," in *Proc. 2016 IEEE Int. Power Electron. Motion Control Conf.*, 2016, pp. 912–917.

[16] B. Hafez, P. Enjeti, and S. Ahmed, "A robust controller for medium voltage ac collection grid for large scale photovoltaic plants based on medium frequency transformers," in *Proc. 2016 IEEE Appl. Power Electron. Conf. Expo.*, 2016, pp. 936–942.

[17] J. Xu, P. Shi, C.-C. Lim, C. Cai, and Y. Zou, "Integrated structural parameter and robust controller design for attitude tracking maneuvers," *IEEE/ASME Trans. Mechatron.*, vol. 21, no. 5, pp. 2490–2498, Oct. 2016.

[18] D. Liu, X. Yang, D. Wang, and Q. Wei, "Reinforcement-learning-based robust controller design for continuous-time uncertain nonlinear systems subject to input constraints," *IEEE Trans. Cybern.*, vol. 45, no. 7, pp. 1372–1385, Jul. 2015.

[19] O. P. Malik and Y. Zeng, "Design of a robust adaptive controller for a water turbine governing system," *IEEE Trans. Energy Convers.*, vol. 10, no. 2, pp. 354–359, Jun. 1995.

[20] B. D. Youn *et al.*, "Resilience allocation for resilient engineered system design," *J. Inst. Control, Robot. Syst.*, vol. 17, no. 11, pp. 1082–1089, 2011.

[21] J. Wang *et al.*, "Toward a resilient holistic supply chain network system: concept, review and future direction," *IEEE Syst. J.*, vol. 10, no. 2, pp. 410–421, Jun. 2016.

[22] J. Li and Z. Xi, "Engineering recoverability: A new indicator of design for engineering resilience," in *Proc. ASME 2014 Int. Design Eng. Tech. Conf. Comput. Inf. Eng. Conf.*, 2014, Paper DETC2014-35005.

[23] Z. Hu and S. Mahadevan, "Resilience assessment based on time-dependent system reliability analysis," *J. Mech. Des.*, vol. 138, no. 11, 2016, Art. no. 111404.

[24] M. Ouyang and Z. Wang, "Resilience assessment of interdependent infrastructure systems: With a focus on joint restoration modeling and analysis," *Rel. Eng. Syst. Saf.*, vol. 141, pp. 74–82, 2015.

[25] Y.-P. Fang, N. Pedroni, and E. Zio, "Resilience-based component importance measures for critical infrastructure network systems," *IEEE Trans. Rel.*, vol. 65, no. 2, pp. 502–512, Jun. 2016.

[26] M. J. Chalupnik, D. C. Wynn, and P. J. Clarkson, "Comparison of ilities for protection against uncertainty in system design," *J. Eng. Des.*, vol. 24, no. 12, pp. 814–829, 2013.

[27] N. Yodo and P. Wang, "Resilience allocation for early stage design of complex engineered systems," *J. Mech. Des.*, vol. 138, no. 9, 2016, Art. no. 091402.

[28] E. Hollnagel, "RAG-The resilience analysis grid," in *Resilience Engineering in Practice: A Guidebook*. Farnham, U.K.: Ashgate, 2011.

[29] C. W. Zobel and L. Khansa, "Characterizing multi-event disaster resilience," *Comput. Oper. Res.*, vol. 42, pp. 83–94, 2014.

[30] N. Yodo and P. Wang, "Resilience analysis for complex supply chain systems using Bayesian networks," in *Proc. 54th AIAA Aerosp. Sci. Meeting*, 2016, Paper AIAA 2016-0474.

[31] D. Henry and J. E. Ramirez-Marquez, "Generic metrics and quantitative approaches for system resilience as a function of time," *Rel. Eng. Syst. Saf.*, vol. 99, pp. 114–122, 2012.

[32] D. G. Dessavre, J. E. Ramirez-Marquez, and K. Barker, "Multidimensional approach to complex system resilience analysis," *Rel. Eng. Syst. Saf.*, vol. 149, pp. 34–43, 2016.
[33] B. M. Ayyub, "Systems resilience for multihazard environments: definition, metrics, and valuation for decision making," *Risk Anal.*, vol. 34, no. 2, pp. 340–355, 2014.
[34] B. M. Ayyub, "Practical resilience metrics for planning, design, and decision making," *ASCE-ASME J. Risk Uncertainty Eng. Syst., Part A: Civil Eng.*, vol. 1, no. 3, 2015, Art. no. 04015008.
[35] M. Ouyang, L. Dueñas-Osorio, and X. Min, "A three-stage resilience analysis framework for urban infrastructure systems," *Struct. Saf.*, vol. 36, pp. 23–31, 2012.
[36] K. H. Ang, G. Chong, and Y. Li, "PID control system analysis, design, and technology," *IEEE Trans. Control Syst. Technol.*, vol. 13, no. 4, pp. 559–576, Jul. 2005.
[37] R. N. Clark, *Control System Dynamics*. Cambridge, U.K.: Cambridge Univ. Press, 1996.
[38] D. Hinrichsen and A. J. Pritchard, *Mathematical Systems Theory I: Modelling, State Space Analysis, Stability and Robustness*, vol. 48. New York, NY, USA: Springer, 2011.
[39] F. J. C. Roger Chiu, D. López-Mancilla, F. G. Peña-Lecona, M. Mora-González, and J. M. Maciel, "Modeling of control systems," in *MATLAB Application for the Practical Engineer*, K. Bennett, Ed. Rijeka, Croatia: InTech, 2014.
[40] D. Christiansen, C. Alexander, and R. Jurgen, *Standard Handbook of Electronic Engineering*. New York, NY, USA: McGraw-Hill, 2005.
[41] G. Bai and P. Wang, "Prognostics using an adaptive self-cognizant dynamic system approach," *IEEE Trans. Rel.*, vol. 65, no. 3, pp. 1427–1437, Sep. 2016.
[42] G. Bai, P. Wang, and C. Hu, "A self-cognizant dynamic system approach for prognostics and health management," *J. Power Sources*, vol. 278, pp. 163–174, 2015.

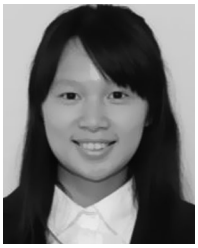

Nita Yodo received the B.S., M.S., and Ph.D. degrees in industrial and manufacturing engineering from Wichita State University, Wichita, KS, USA, in 2011, 2013, and 2017, respectively.

She is currently an Assistant Professor in the Department of Industrial and Manufacturing Engineering, North Dakota State University, Fargo, ND, USA. Her research interests include designing resilient and sustainable engineered systems.

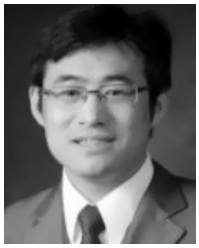

Pingfeng Wang (M'09) received the B.E. degree in mechanical engineering from The University of Science and Technology, Beijing, China, in 2001, the M.S. degree in applied mathematics from Tsinghua University, Beijing, China, in 2006, and the Ph.D. degree in mechanical engineering from the University of Maryland, College Park, MD, USA, in 2010.

He is currently an Associate Professor in the Department of Industrial and Enterprise Systems Engineering, University of Illinois at Urbana-Champaign, Urbana, IL, USA. His dedicated research efforts have resulted in more than 100 publications in refereed journals and conference proceedings. His research interests include engineering system design for reliability, failure resilience and sustainability, and prognostics and health management.

Dr. Wang's research has garnished him notable international awards including two times ASME Best Paper Awards in 2008 and 2013, respectively, 2012 IEEE PHM Best Paper Award, the National Science Foundation CAREER Award in 2014, the Young Researcher Award from the International Society of Green Manufacturing and Applications in 2012, and the Design Automation Young Investigator Award from the American Society of Mechanical Engineers in 2016.

Melvin Rafi received the B.S. and M.S. degrees in aerospace engineering in 2007 and 2013, respectively, from Wichita State University, Wichita, KS, USA, where he is currently working toward the Ph.D. degree in the Department of Aerospace Engineering.

He is working as a Graduate Research Assistant in the General Aviation Flight Laboratory, Wichita State University. His research interests currently include intelligent adaptive control, loss-of-control prediction systems for aircraft, and augmented-reality assistive displays for pilot use.